16TH EUROPEAN CONFERENCE ON EARTHQUAKE ENGINEERING THESSALONIKI 18 - 21 JUNE 2018

SEISMIC RESPONSE OF BRIDGE COLUMNS WITH HIGH-PERFORMANCE MATERIALS

Farshid HOSSEINI[1], Bora GENCTURK[2]

ABSTRACT

Recently, the use of high-performance fiber-reinforced concrete (HPFRC) and superelastic alloys (SEAs) in bridge columns have been investigated to mitigate the damage and reduce or eliminate the permanent deformations. The HPFRC studied in this research uses synthetic fibers in a mortar base and has high ductility in tension and high energy absorption characteristics under cyclic loading. The SEAs are Cu-based and show strain recovery (pseudo-yielding) behavior up to approximately 12% strain. A series of tests have been conducted by the same authors in a previous study where bridge columns with a HPFRC hollow section, a concrete core, and Cu-based SEAs as the plastic hinge reinforcement was investigated. The results indicated that the use of a HPFRC hollow section is as efficient as making the entire cross-section from HPFRC. Similarly, it was shown that with different amounts of steel rebar replacement in the plastic hinge region, Cu-based SEAs could effectively be used to compromise between reducing permanent deformation and increasing energy dissipation. In this study, computational models of this bridge column concept are created to better understand the seismic response of this new column concept. A commercially available finite element package has been modified to capture the constitutive behavior of HPFRC and Cu-based SEAs. High-fidelity 3D computational models of columns have been developed capturing the key features of degradation including material softening and bond behavior. Very good correlations were obtained between the experiments and computer simulations.

Keywords: Finite element analysis, engineered cementitious composites (ECC), Cu-Al-Mn superelastic alloys, bridge columns, seismic performance

1. INTRODUCTION

A functional transportation network in the aftermath of a major disaster is essential for quick response and initiation of recovery process. Recent strong earthquakes have shown that the conventional reinforced concrete (RC) bridge columns are susceptible to large permeant deformations and considerable damage because of yielding of the longitudinal reinforcement as the main mechanism of dissipating energy, and poor performance of conventional concrete under cyclic loads. Using high-performance materials such as high-performance fiber reinforced concrete (HPFRC) and superelastic alloys (SEA) has recently received significant attention by researchers to address these issues. Engineered cementitious composite (ECC) is a special type of HPFRC which exhibits high tensile ductility and deformability in addition to multiple distributed fine cracks under both quasi-static and dynamic loads (Li, 1992; Li et al., 2001; Maalej et al., 2005). Furthermore, ECC has superior durability and shear resistance compared to conventional concrete (Li, 2008; Boshoff, 2014; Gideon & Zijl, 2007). Superelasticity refers to recovery of inelastic deformations upon stress removal which is observed in shape memory alloys (SMAs) in austenite phase under operating temperature (DesRoches et al., 2004). The Efficiency of ECC and SEAs in reducing the permanent deformation and damage in bridge columns has been demonstrated through several experimental programs (Noguez et al., 2011; Saiidi et al., 2009; Saiidi & Wang, 2006; Nakashoji & Saiidi, 2014; Hosseini et al., 2016). However, most of the studies

[1]PhD Candidate, Sonny Astani Department of Civil and Environmental Engineering, University of Southern California, Los Angeles, California, USA, hosseini.seyyedfarshid@gmail.com.
[2]Assistant Professor, Sonny Astani Department of Civil and Environmental Engineering, University of Southern California, Los Angeles, California, USA, gencturk@usc.edu.

concentrated on application of NiTi SEA bars, some along with ECC in the potential plastic hinge region of the bridge columns. Prohibitively high cost, machinability issues, particularly related to drilling and threading, and deterioration of superelasticity in low temperatures are some of the obstacles in structural application of NiTi SEAs (Zhang et al., 2008). On the other hand, the performance of Cu-Al-Mn SEA bars have continuously been improved in the recent years to tackle these issues and facilitate utilization of Cu-based SEAs in structures through manufacturing large diameter bars with comparable superelasticity (Araki et al., 2011; Omori et al., 2013). To improve durability of bridge columns in addition to their seismic performance, an innovative bridge column design was proposed by the authors in an earlier study (Hosseini et al., 2016). The design concept consists of a prefabricated reinforced ECC (RECC) hollow section embedded in a RC foundation and filled with conventional concrete. The longitudinal reinforcement is partially replaced with Cu-Al-Mn SEA bars at the potential plastic hinge region to reduce the permanent deformations due to strong earthquakes. The previously conducted experiments revealed that the proposed design concept enhances damage tolerance, considerably reduces the permanent deformations due to incremental cyclic deformations, and can be adapted to optimize use of high-performance materials yet expensive in bridge columns (Hosseini et al., 2016). In this study, numerical models of the tested specimens are developed and the results are validated against the experimental data. Despite sufficiency of the employed numerical modeling approach in this study in predicting the global behavior of the bridge columns with high-performance materials, it should be noted that the modeling approach is unable to consider concrete spalling and rupture of the reinforcement, which were observed during the tests for conventional columns.

2. SUMMARY OF EXPERIMENTAL PROGRAM

The geometry of the tested specimens is presented in Figure 1. The column included a prefabricated RECC hollow section consisting of the longitudinal and transverse reinforcement. The RECC hollow section had an outer and an inner diameter of 203.2 mm and 127 mm, respectively. After prefabrication of the RECC hollow section using a high fly ash content ECC admixture (HFA), it was embedded inside a RC foundation and a RC cap was built on top of the column to transfer the loads from the loading units to the specimen. Eight evenly distributed reinforcing bars (two 12.7 mm at the neutral axis and six evenly distributed 9.5 mm rebar) provided a longitudinal reinforcement ratio of 2%. The transverse reinforcement consisted of 3.9 mm galvanized wire in spiral form with pitch of 32 mm yielding a transverse reinforcement ratio of 0.64%. To replace the longitudinal reinforcement with SEAs, Cu-Al-Mn SEA bars were machined in dog-bone shape and threaded at the two ends; then connected to the longitudinal reinforcement using custom made mechanical couples. The Cu-Al-Mn SEA bars were embedded 66 mm in the foundation and debonded from the surrounding material using a tape. The prepared specimens were tested under 100 kN constant axial load (approximately 7.5% of squash capacity) and reversed cyclic lateral displacements up to 9.5% drift. A state of the art testing unit capable of applying loads and deformations in all six degrees of freedom was used to apply the loads. Detailed information about the geometry, the construction process, the test setup, the material properties, and the experimental results is available in Hosseini et al. (2016). Two of the configurations, HFA-Tube and HFA-Tube-SEA, see Figure 1, are investigated numerically in this paper. There was no Cu-Al-Mn SEA bars in HFA-Tube while six Cu-Al-Mn SEA bars were used in the longitudinal reinforcement of the HFA-Tube-SEA in the plastic hinge region. Damaged was observed in the form of multiple fine cracks and a single large crack in HFA-Tube and HFA-Tube-SEA, respectively, without any sign of spalling of the cover concrete unlike the control RC specimen. This observation indicated considerable enhancement in the damage tolerance of the bridge columns by application of ECC due to its tensile strain-hardening behavior. Additionally, permanent deformations decreased by about 90% in the HFA-Tube-SEA compared to the control RC specimen because of superelastic behavior of the Cu-Al-Mn SEA bars. However, energy absorption capacity of HFA-Tube-SEA declined 63% compared to the control RC specimen emphasizing special considerations, such as increasing the longitudinal reinforcement ratio, in bridge columns with high number of Cu-Al-Mn SEA bars to compensate for the loss of energy absorption capacity. Even though, incorporating ECC enhanced the ultimate lateral strength of HFA-Tube, around 10%, its energy absorption capacity and permanent deformations decreased around 12% and 15%, respectively, compared to the control RC specimen. These reductions

in the energy absorption capacity and permanent deformations was a result of superior bonding between the longitudinal reinforcement and ECC, which resulted in a longer plastic hinge and limited the maximum post-yield strains in the rebar (Hosseini et al., 2016).

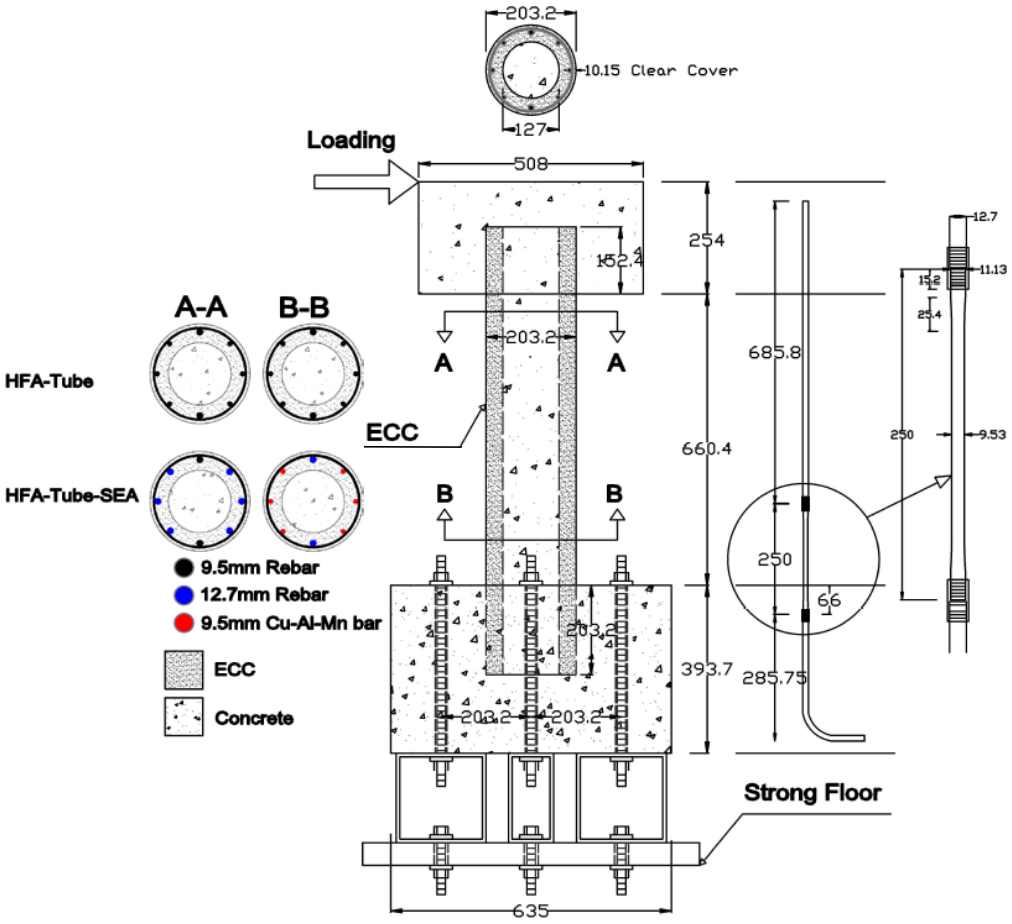

Figure 1. Geometry of the tested specimens (dimensions are in mm)

3. MODELING APPROACH

3.1 Constitutive Modeling of High-Performance Materials

ATENA (Bures et al., 2017), a commercial finite element modeling (FEM) package, was used to conduct the numerical modeling of the tested columns. The incorporated material constitutive models are presented in this section.

CC3DNonLinCementitious2 material model from ATENA (Bures et al., 2017) material library was employed to simulate cyclic behavior of concrete and ECC. The results of uniaxial compression tests were used to generate a default concrete constitutive model which was then adjusted for cyclic loads. The modeling approach for ECC is illustrated in Figure 2. To simulate tensile behavior of ECC, the concrete constitutive model was merged with smeared reinforcement and the mechanical properties of the smeared reinforcement was adjusted to capture the tensile strain-hardening behavior of ECC, see Figure 2(A). The modeling approach was validated through numerical modeling of the tested dog-bone specimens and matching the numerical and experimental results, Figure 2(B) and Figure 2(C). Additionally, a single brick element, see Figure 2(D), was modeled with the developed ECC material model and subjected to reversed cyclic tensile-compressive loads to ensure sufficiency of the model for cyclic loads, see Figure 2(E). As shown in Figure 2, the material model could sufficiently capture the main characteristics of behavior of ECC.

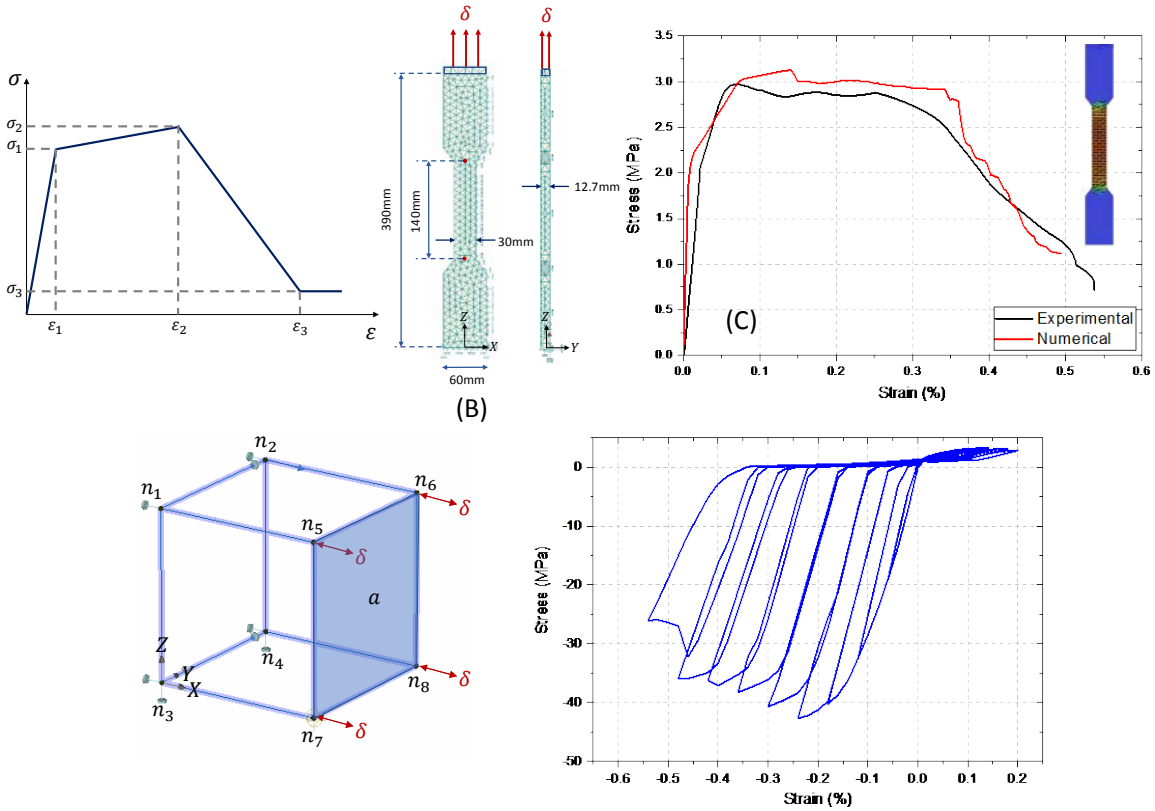

Figure 2. ECC modeling approach: (A) schematic stress-strain behavior of smeared reinforcement, (B) modeled dog-bone specimen, (C) stress-strain diagram for modeled dog-bone specimen, (D) single brick element, (E) stress-strain response from brick elements under to cyclic loads

"Cyclic Reinforcement" material from the material library was used in bilinear form to simulate behavior of both longitudinal and transverse reinforcement. Experimental results were used for the elastic modulus, 180,000 MPa, and yield stress, 423 MPa, while the default values were taken for the parameters of Menegotto and Pinto model and Bauschinger effect. Same material model was considered for the transverse reinforcement since experimental data was unavailable.

To simulate cyclic behavior of Cu-Al-Mn SEA bars, a one-dimensional constitutive model was implemented based on Motahari & Ghassemieh (2007), see Figure 3(A). Upon implementation, a single bar element was modeled and subjected to cyclic loads to calibrate the constitutive model using the experimental data, see Figure 3(B).

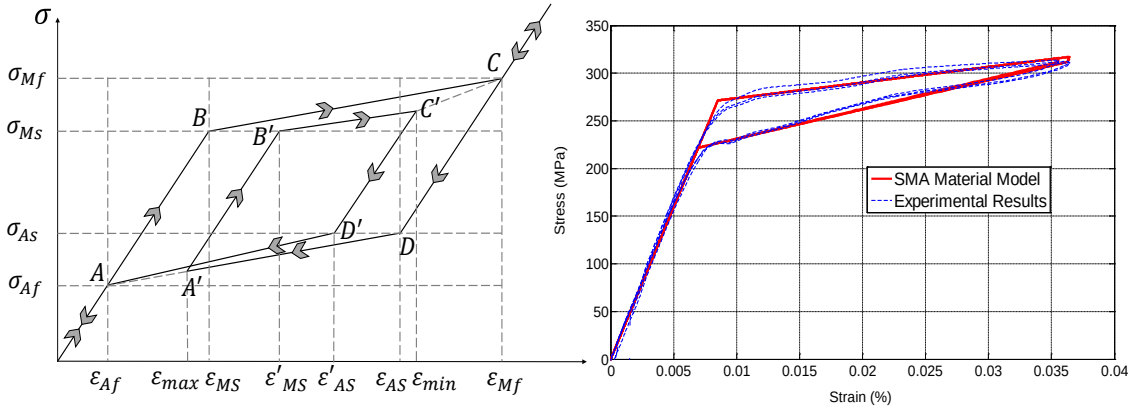

Figure 3. Constitutive model for SEA: (A) theoretical behavior, (B) calibrating the model with experimental data

As it can be seen, the developed constitutive model could predict the superelastic behavior of Cu-Al-Mn SEA bars accurately in terms of elastic modulus, yield stress, post-yield modulus, and unloading characteristics.

"Memory Bond" material based on the bond model by Bigaj (1999) was used to simulate bond characteristics of the longitudinal reinforcement. The general behavior of the "Memory Bond" material and the defined bond models are presented in Figure 4. A significantly weak bond was generated to simulate debonding in Cu-Al-Mn bars. The unloading pass parameter, τ_1, was equal to 4.42 MPa and 0.48 MPa for the regular and weak bonds, respectively.

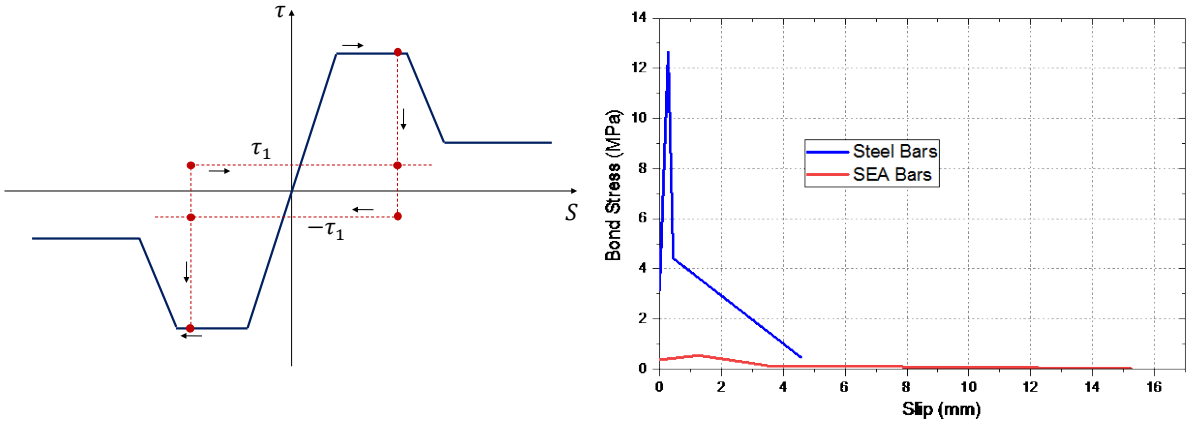

Figure 4. "Memory Bond" material: (A) general cyclic behavior, (B) bond-slip diagrams for reinforcing steel and Cu-Al-Mn SEA bars

3.2 Finite Element Models

The numerical models were created to ensure accurate representation of the actual tested specimens. The developed numerical models are illustrated in Figure 5. The specimens were modeled in three separate parts: (i) top cap, (ii) foundation, and (iii) column. The RECC hollow section was created using multi-sided column option with 12 sides with a multi-sided opening. The concrete core was created separately and then placed inside the RECC hollow section assuming displacement compatibility at the shared nodes, i.e., perfect connection. Upon generating the geometry of the column, the end caps were created consisting of openings to a certain depth to embed the column. Finally, the column, the foundation, and the top cap were connected to each other with perfect contacts at the corresponding common surfaces. Additionally, elastic steel plates were placed atop of the top cap and underneath of the foundation to distribute the axial loads and simulate the strong floor, respectively. Linear line springs were added along the two edges of the foundation and perpendicular to the lateral load direction to simulate the effect of the test setup flexibility observed during the experimental program. Further, the center line of the elastic plate underneath the foundation was fixed in the three global directions to simulate the interaction between the strong floor and the foundation. Finally, the out-of-plane deformations were restricted by restraining the corresponding degree of freedom in the top elastic plate, see Figure 5(A).

Longitudinal and transverse reinforcement were created using one-dimensional elements. The distance between the transverse stirrups was doubled and the corresponding area was increases accordingly to reach a similar transverse reinforcement ratio as the tested specimens while reducing number of the elements in the numerical model. To reduce the required memory and the computational cost, 3% smeared reinforcement was applied to both the top cap and the foundation in the three main global

directions instead of discrete reinforcing bars, Figure 5(A). In HFA-Tube-SEA specimen, the longitudinal bars were divided to three segments and the implemented Cu-Al-MN SEA constitutive model was assigned to the middle sections. The SEA bars were debonded by applying the weak bond while restricting the slip at the two ends. To satisfy continuity in the bond model, perfect bond condition was applied to the top and bottom segments of the longitudinal reinforcement with Cu-Al-Mn SEA bar in the middle, Figure 5(B). However, regular bond model was considered for the longitudinal reinforcement in the HFA-Tube specimens. It should be noted that the transverse reinforcement had perfect bond with the surrounding material in both numerical models.

Linear tetrahedral elements with four nodes and reduced integration points were used to mesh the entire specimen, Figure 5(C). A maximum mesh sizes of 0.04 m and 0.1 m were considered for the column and the end caps, respectively. Standard Newton-Raphson solution method was employed to analyze the model under distributed axial load and cyclic lateral displacement with 0.0167% drift increment in each load step, Figure 5(C).

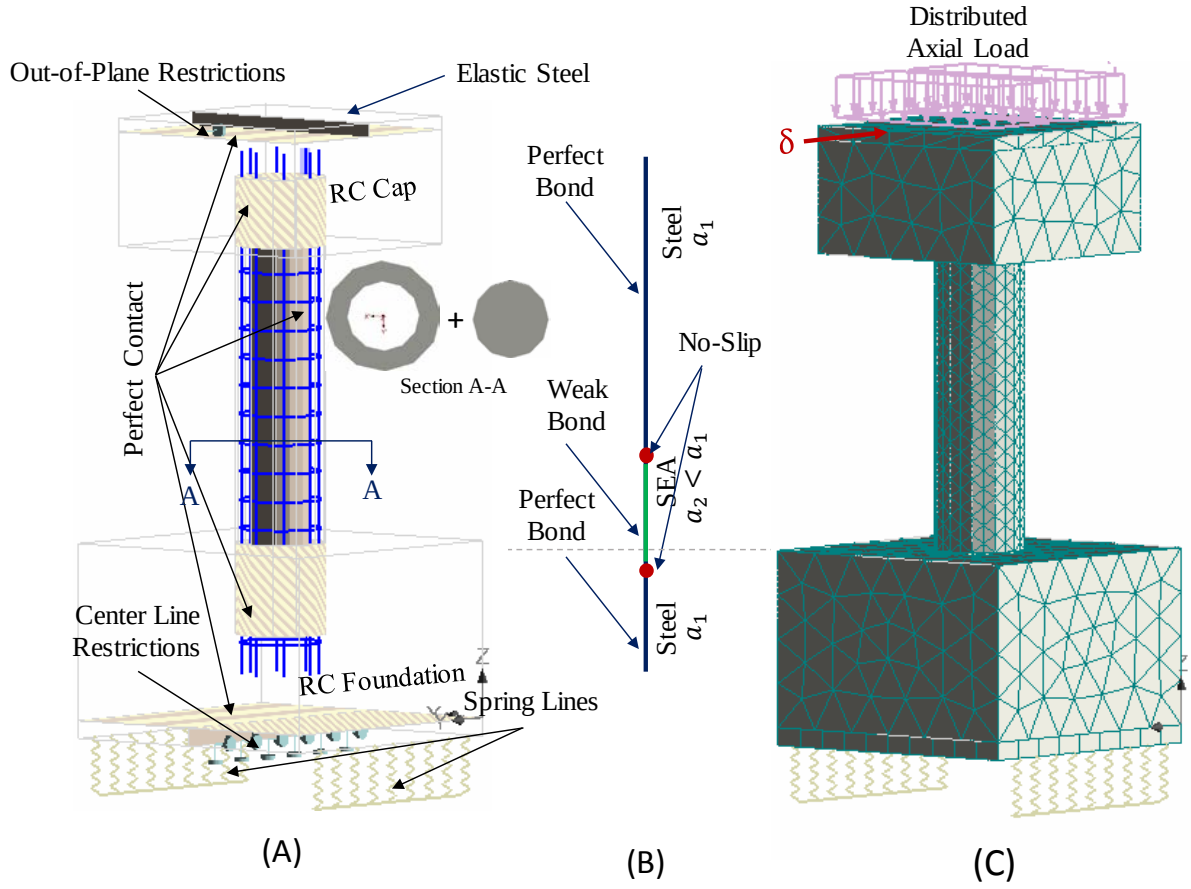

Figure 5. Numerical models: (A) geometry, reinforcement, and boundary condition, (B) modeling of Cu-Al-Mn SEA bars and steel rebar, (C) mesh and loading

4. RESULTS AND DISCUSSION

The load-deformation diagrams obtained from the numerical models are compared with the experimental data in Figure 6. As seen, the numerical models could accurately predict the cyclic behavior of the both specimens (with and without Cu-Al-Mn SEA bars in the potential plastic hinge region) in terms of ultimate lateral strength, post-peak behavior, and permanent deformations.

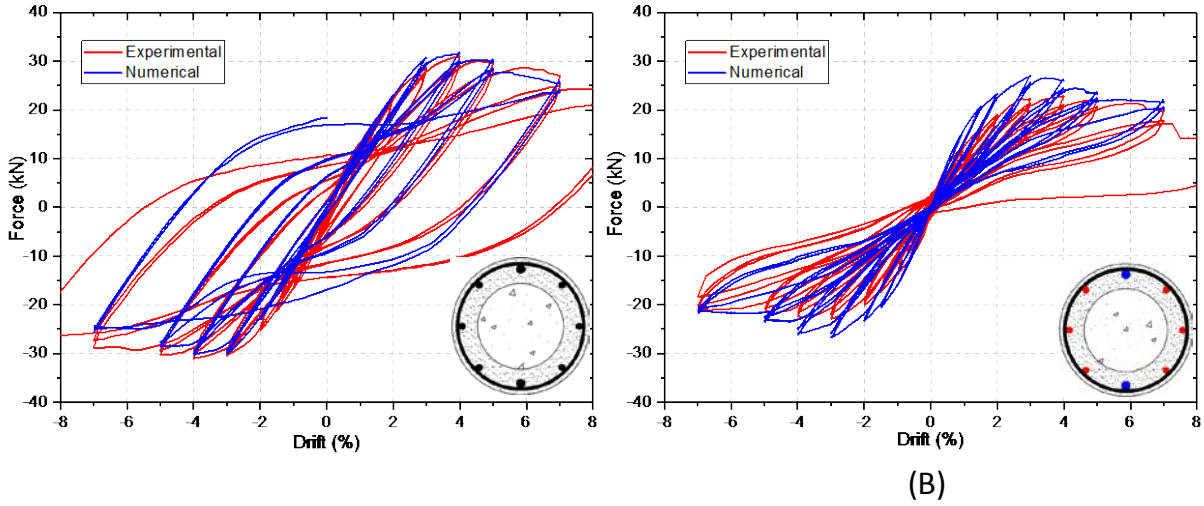

Figure 6. Load-deformation diagrams: (A) HFA-Tube, (B) HFA-Tube-SEA

To quantitatively compare the performance of the developed models, several measures including load and drifts at maximum, ultimate, and yield points were defined using average of the push and pull envelope curves, see Figure 7(A). The defined maximum point corresponds to the maximum lateral strength of the column in the load-deformation diagram, the ultimate point corresponds to the 15% drop in the load carrying capacity of the column in the softening branch of the average envelop curve while the yield point was calculated based on the reduced stiffness equivalent elasto-plastic method of Park (1988). Additionally, energy absorption capacity, E_0, and permanent deformation, δp, were defined based on the hysteresis response of the columns, see Figure 7(B). The absorbed energy was defined as the area inside the hysteresis curves up to completion of the 7% peak drift. Correspondingly, the permanent drift considered as the average of the permanent deformations in pull and push directions in last cycle of the 7% drift.

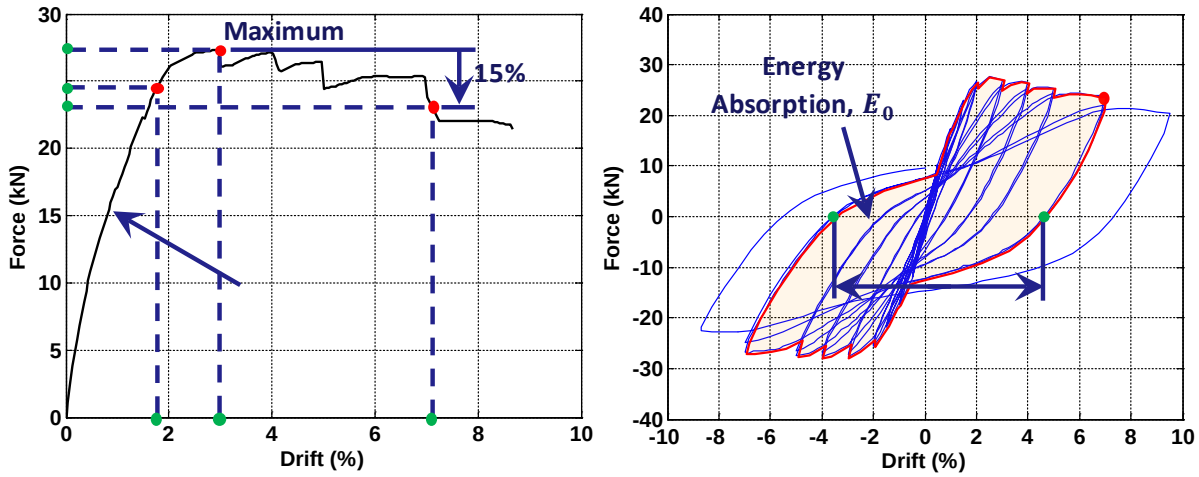

Figure 7. Definition of measures for quantitate comparison.

Table 1 summarizes the corresponding values for the defined measures obtained from the experiments and numerical simulations. As seen in Table 1, the numerical models could predict the force related measures better than those related to the deformation which is attributed to insufficiency of the numerical models in capturing the rupture of Cu-Al-Mn SEA rebars, performance of the concrete constitutive model under cyclic loads, and estimating the deformations in the test setup using the line springs.

Table 1: Comparing numerical and experimental results.

Specimen	HFA-Tube			HFA-Tube-SEA		
	Exp.	FEM	Error (%)	Exp.	FEM	Error (%)
Drift at Yield, δ_y (%)	2.94	2.72	-7.48	2.28	1.99	-12.7
Yield Force, F_y (kN)	27.2	28.69	5.48	20.1	22.96	14.23
Drift at Maximum, δ_m (%)	4.01	3.97	-1.00	4.00	2.99	-25.3
Maximum Force, F_m (kN)	30.26	30.77	1.69	22.83	26.76	17.21
Drift at Ultimate, δ_u (%)	7.15	5.02	-29.8	7.01	5	-28.7
Ultimate Force, F_u (kN)	25.72	26.16	1.71	19.41	22.75	17.21
Permanent Drift, δ_p (%)	3.63	4.37	20.39	0.37	0.19	-48.7
Energy Abs., E_a (kN-m)	8.36	9.31	11.36	3.43	2.16	-37.0

Further investigations confirmed limited effect of increasing the distance between the lateral reinforcement on the response of the column up to 7% drift, which is the target drift in the analysis, see Figure 8. Considering flexural dominant behavior of the bridge columns, longitudinal reinforcement had the main contribution in the cyclic response. Therefore, confinement from the transverse reinforcement had negligible effect on the overall behavior of the columns. Additionally, buckling of the longitudinal reinforcement was less of concern in increasing the spacing of the transverse reinforcement since it was restrained by the surrounding ECC.

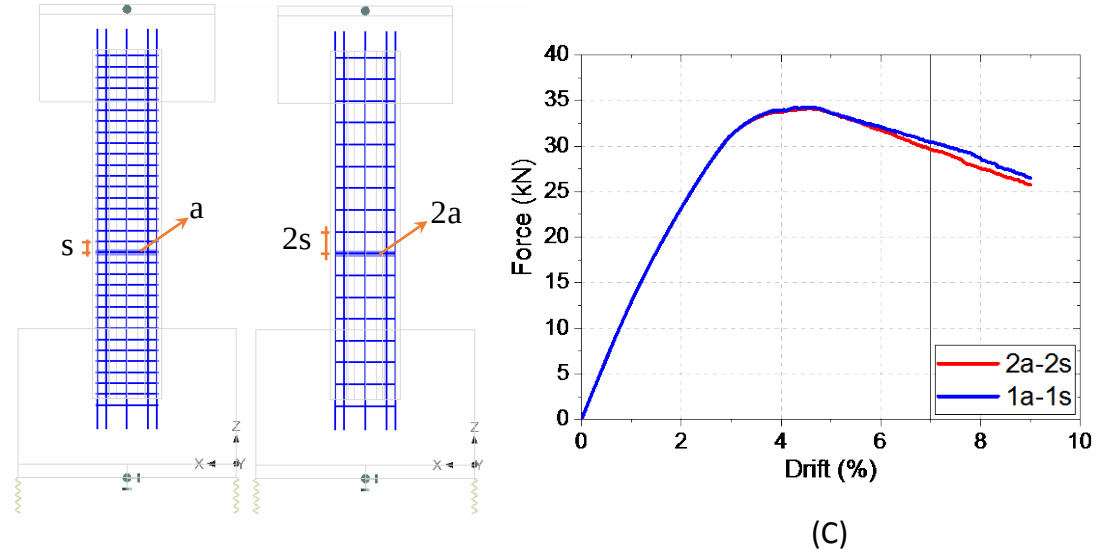

Figure 8: Effect of spacing of transverse reinforcement in HFA-Tube: (A) actual spacing (1a-1s), (B) doubled spacing with doubled reinforcement area (2a-2s), (C) load-deformation diagrams.

5. CONCLUSIONS

In this paper, innovatively designed bridge columns are modeled and the results are compared with the experimental data. The design utilizes high-performance materials in an innovative way to enhance the damage tolerance and reduce the permanent deformations of bridge columns due to strong earthquakes. The main findings of this study are listed below:

- Unique characteristics of ECC were successfully simulated by implementing smeared reinforcement in a concrete constitutive model. Several characteristics of ECC including the strain-hardening and the strain-softening behavior were captured using this approach.

- Superelastic behavior of Cu-Al-Mn SEA bars was successfully predicted using one-dimensional elements suitable for RC structural members as longitudinal reinforcement.
- The numerical models could accurately predict the cyclic performance of the innovative bridge columns in terms of the permanent deformation, the ultimate lateral strength, the post-peak behavior, and the energy absorption capacity.
- The numerical model of HFA-Tube-SEA was unable to capture the rupture of the Cu-Al-Mn SEA bars observed in the experimental program, which resulted in considerable difference with the experimental results in terms of the energy absorption capacity and the permanent drift after rupture of the Cu-Al-Mn SEA bars.

6. ACKNOWLEDGMENTS

The funding for this research was provided by the United States National Science Foundation under the award no. 1642488. The findings presented here are those of the authors and do not necessarily reflect the opinion of the sponsor.

7. REFERENCES

Araki, Y., Endo, T., Omori, T., Sutou, Y., Koetaka, Y., Kainuma, R., & Ishida, K. (2011). Potential of superelastic Cu–Al–Mn alloy bars for seismic applications. *Earthquake Engineering and Structural Dynamics, 40*(1), 107-115.

Bigaj, A. J. (1999). Structural dependence of rotation capacity of plastic hinges in RC beams and slabs, *Ph.D. Thesis*, Senior Scientist Integrator, Center for Technical Sciences, The Hague, Netherlands.

Boshoff, W. P. (2014). Cracking behavior of strain-hardening cement-based composites subjected to sustained tensile loading. *ACI Materials Journal, 111*(5).

Bures, P., Cervenka, J., Cervenka, V., Jendele, L. J., Pukl, R., & Smrz, O. (2017). *ATENA-Advanced Tool for Engineering Nonlinear Analysis* (5.3.4 ed.). Na Hrebenkach: Consulting Červenka.

DesRoches, R., McCormick, J., & Delemont, M. (2004). Cyclic properties of superelastic shape memory alloy wires and bars. *Journal of Structural Engineering, 130*(1), 38-46.

Gideon, P., & Zijl, v. (2007). Improved mechanical performance: shear behaviour of strain-hardening cement-based composites (SHCC). *Cement and Concrete Research, 37*, 1241-1247.

Hosseini, F., Gencturk, B., Lahpour, S., & Ibague Gil, D. (2016). An experimental investigation of innovative bridge columns with engineered cementitious composites and Cu–Al–Mn super-elastic alloys. *Smart Materials and Structures, 24*(8), 085029.

Li, V. C. (1992). Performance driven design of fiber reinforced cementitious composites. *Fiber Reinforced Cement and Concrete*. London: E & FN Spon.

Li, V. C. (2008). Engineered cementitious composites (ECC) – material, structural, and durability performance. In *Concrete Construction Engineering Handbook* (p. Chapter 24). CRC Press.

Li, V. C., Wang, S., & Wu, C. (2001). Tensile strain-hardening behavior of polyvinyl alcohol engineered cementitious composite (PVA-ECC). *Materials Journal, 98*(6), 483-492.

Maalej, M., Quek, S. T., & Zhang, J. (2005). Behavior of hybrid-fiber engineered cementitious composites subjected to dynamic tensile loading and projectile impact. *Journal of Materials in Civil Engineering, 17*(2), 143-152.

Motahari, S. A., & Ghassemieh, M. (2007). Multilinear one-dimensional shape memory material model for use in structural engineering applications. *Engineering Structures*, 904–913.

Nakashoji, B. A., & Saiidi, S. (2014). Seismic performance of square nickel-titanium reinforced ECC columns with headed couplers. Reno, NV: Center for Civil Engineering Earthquake Research Report CCEER-14-05, Univ. of Nevada.

Noguez, C., A., C., & Saiidi, M. S. (2011). Shake-table studies of a four-span bridge model with advanced materials. *Journal of Structural Engineering, 138*(2), 183-192.

Omori, T., Kusama, T., Kawata, S., Ohnuma, I., Sutou, Y., Araki, Y., Kainuma, R. (2013). Abnormal grain growth induced by cyclic heat treatment. *Science, 341*(6153), 1500-1502.

Park, R. (1988). Ductility evaluation from laboratory and analytical testing. *The 9th World Conference on Earthquake Engineering.* Tokyo-Kyoto, Japan.

Saiidi, M. S., & Wang, H. (2006). Exploratory study of seismic response of concrete columns with shape memory alloys reinforcement. *ACI Structural Journal, 103*(3), 436.

Saiidi, M. S., O'Brien, M., & Sadrossadat-Zadeh, M. (2009). Cyclic response of concrete bridge columns using superelastic Nitinol and bendable concrete. *ACI Structural Journal, 106*(1), 69.

Zhang, Y., Camilleri, J. A., & Zhu, S. (2008). Mechanical properties of superelastic Cu–Al–Be wires at cold temperatures for the seismic protection of bridges. *Smart Materials and Structures, 17*(2).